Uncovering Molecular Insights into Blood–Brain Barrier Dysfunction in Alzheimer's Disease

Konstantinos Lazaros*, Marios G. Krokidis, Gerasimos Grammenos, Styliani Adam,
Themis P. Exarchos, Panagiotis Vlamos and Aristidis G. Vrahatis
Bioinformatics and Human Electrophysiology Laboratory,
Department of Informatics, Ionian University, 49100, Corfu, Greece
Corresponding author: lakonstant@ionio.gr

2025 IEEE 25th International Conference on Bioinformatics and Bioengineering (BIBE) | 979-8-3315-5899-4/25/$31.00 ©2025 IEEE | DOI: 10.1109/BIBE66822.2025.00013

***Abstract*—Alzheimer's disease (AD) is a progressive neurodegenerative disorder primarily linked to memory loss and cognitive decline, although less common clinical manifestations are being more frequently identified. Disruptions in gene expression and regulation have been increasingly linked to neurodegeneration. Single-cell RNA sequencing (scRNA-seq) and single-nucleus RNA sequencing (snRNA-seq) are powerful methods for analyzing transcriptomic diversity at the level of individual cells. Herein, analysis of snRNA-seq data derived from the entorhinal cortex of post-mortem brain samples from individuals either diagnosed with AD (Braak stage II) or serving as healthy controls was executed trying to identify potent biomarkers and molecular mechanisms in which these genes are involved. Preprocessing, integration, clustering and cell type annotation were performed using indicator-based methods followed by differentially expression analysis and enrichment analysis. UMAP was used for data visualization as well as Local Inverse Simpson's Index to evaluate the effectiveness of data integration. Leiden clustering was performed on the integrated dataset while the Wilcoxon rank-sum test was utilized for differential expression analysis. Cell-cell junctions were detected as the most significantly enriched category showing significant contribution to the structural integrity and signaling across the blood-brain barrier. Moreover, important pathways such as the Brain-Derived Neurotrophic Factor and L-glutamate transmembrane transport were detected emphasizing the role of synaptic dysfunction and neurodegeneration in AD. This approach supports the implementation of snRNA-seq data analysis in complex disorders such as neurodegenerative diseases, providing new challenges for identifying fundamental biological processes on a molecular perspective.**

***Index Terms*—Alzheimer's disease, scRNA-seq, snRNA-seq, RNA sequencing, Differentially Expressed Genes, Data Integration, Molecular Pathways**

I. Introduction

Alzheimer's disease (AD) is a progressive neurodegenerative disorder that primarily affects individuals over the age of 65, leading to a gradual decline in memory, cognitive functions, and the ability to carry out everyday tasks [1]. The earliest neural damage typically occurs in the hippocampus [2] and the entorhinal cortex [3], regions critical for memory formation and retrieval. As the disease advances, neuronal loss extends to additional brain areas, resulting in widespread brain atrophy and severe cognitive impairment. Rather than being caused by a single genetic mutation, it is believed to be associated with multiple genetic variants that either increase or reduce the risk of developing the disease.

In recent years, advances in molecular biology and gene expression technologies such as RNA sequencing (RNA-seq) and single-cell RNA sequencing (scRNA-seq) have significantly deepened the understanding of complex diseases like Alzheimer's [4]. scRNA-seq, in particular, enables the analysis of gene expression at single-cell resolution, offering a detailed view of cellular heterogeneity by measuring mRNA expression levels across hundreds to thousands of genes per cell. This allows researchers to uncover previously unrecognized cell subpopulations, reconstruct developmental trajectories, and model transcriptional dynamics, while also providing insights into gene co-regulation, regulatory networks, and transcriptional variation [5]. Complementary to this, single-nucleus RNA sequencing (snRNA-seq) focuses on RNA extracted from isolated nuclei rather than whole cells, making it especially valuable for studying archived or frozen tissues, as well as cells that are difficult to dissociate such as neurons and adipocytes [6].

Despite their strengths, both scRNA-seq and snRNA-seq present several notable challenges. Both technologies typically require more starting material than bulk RNA-seq, making experiments more costly and less feasible when working with limited biological samples. While they offer advantages in analyzing archived or hard-to-dissociate tissues, such as frozen brain samples, also generates highly complex and large-scale datasets [7]. In both cases, the volume and intricacy of the data create significant demands in terms of storage, processing, and interpretation. To address these challenges and ensure the efficient and accurate analysis of such data, specialized computational algorithms (many of which are grounded in artificial intelligence and machine learning methodologies) are essential. Such approaches are particularly well-suited to managing the high-dimensionality and heterogeneity inherent in these datasets, enabling researchers to extract meaningful biological insights from complex cellular landscapes.

The aim of this study is to analyze single-nucleus RNA sequencing (snRNA-seq) data derived from the entorhinal cortex of post-mortem brain samples from individuals either diagnosed with AD (Braak stage II) or serving as healthy controls. The analysis focuses on identifying genes that are significantly over- or under-expressed between the two groups, with the goal of uncovering the molecular pathways and mechanisms in which these genes are involved.

2471-7819/25/$31.00 ©2025 IEEE
DOI 10.1109/BIBE66822.2025.00013

II. Materials and Methods

Given the increasing need for advanced computational approaches to analyze large-scale single-cell RNA sequencing (scRNA-seq) data, this study presents a tailored computational pipeline designed to process and analyze gene expression data related to Alzheimer's disease (AD). The pipeline specifically addresses the complexity of scRNA-seq and snRNA-seq datasets, enabling the identification of potential biomarkers and molecular mechanisms linked to disease progression. The analysis is based on snRNA-seq data from post-mortem brain tissue, available through the Gene Expression Omnibus (GSE147528) [8]. This study profiled the caudal entorhinal cortex and superior frontal gyrus (SFG) across Braak stages of AD. For the purposes of the present analysis, only samples from the SFG were selected, focusing on stages 0 and 2 to ensure computational feasibility and a balanced comparison between control and early-stage disease.

Prior to further analysis, all data batches underwent a standardized preprocessing step to filter out low-quality cells and genes, ensuring that only high-integrity data were retained. A total of seven batches, three corresponding to Braak stage 0 and four to stage 2, were used to examine gene expression differences between early Alzheimer's pathology and healthy controls. All processing and analytical steps were implemented in Python using the Scanpy library [9].

Doublet identification is a key preprocessing step in scRNA-seq and snRNA-seq analyses, aimed at detecting instances where two cells are incorrectly captured as one, leading to artificial gene expression profiles that can mislead downstream analyses [10]. In this study, doublets were identified and removed using SOLO, a neural network-based tool that accurately detects and filters out such artifacts to ensure the quality and reliability of the dataset [11].

Moreover, to account for batch variation and ensure that technical noise did not obscure underlying biological signals, data integration was performed using scVI. This deep learning model, built on a variational autoencoder framework, creates a shared latent representation of the data, enabling more accurate and biologically meaningful downstream analyses [12].

Following batch effect correction, the Leiden algorithm was applied to the data to perform clustering and identify transcriptionally distinct cell populations. As an improved version of the Louvain method, Leiden ensures more robust and well-connected communities by iteratively refining partitions until a stable clustering solution is reached [13].

Cell type annotation was performed using decoupleR [14], a marker-based approach that leverages known marker genes to identify specific cell types. These marker genes were curated from CellMarker 2.0 [15], a comprehensive database of manually annotated cell-type-specific markers. To identify genes with significant expression differences between cell types, a Wilcoxon rank-sum test was applied. From this analysis, the most statistically significant DEGs were selected and subjected to functional enrichment analysis using the Enrichr tool [16] to explore their associated biological pathways and processes.

In addition to the global differential expression and enrichment analyses performed across all annotated cell types, a more focused cell-type-specific approach was conducted to enhance biological resolution. Specifically, endothelial and pericyte cell clusters (which are considered key components of the blood–brain barrier (BBB)) were isolated based on their marker expression following cell-type annotation. Independent differential expression analyses were then performed within each of these two cell populations, followed by functional enrichment analysis using the same statistical and computational tools and parameters as described above. This focused analysis aimed to uncover molecular pathways specifically associated with BBB dysfunction in Alzheimer's disease by highlighting transcriptomic alterations unique to endothelial and pericyte cells. Figure 1 illustrates the analysis workflow implemented in this study.

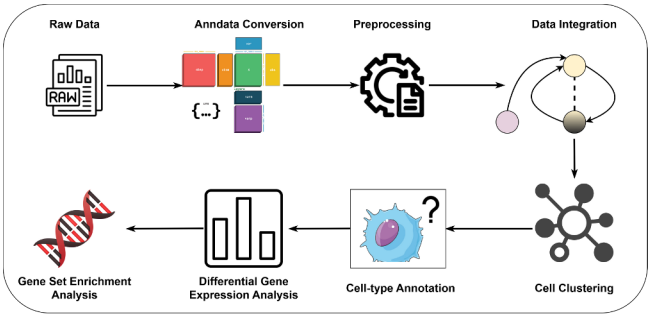

Fig. 1. Overview of the single-cell RNA-seq analysis pipeline used in this study. Raw data are processed and converted to AnnData format, followed by preprocessing, integration, and clustering. Cell types are annotated using marker-based methods, and differentially expressed genes are identified via Wilcoxon rank-sum testing. The top genes are then used for enrichment analysis to uncover relevant biological pathways.

III. Results and Discussion

After preprocessing and merging, the dataset comprised 12,616 cells and 19,965 genes/features. Data visualization was performed using UMAP, a widely used non-linear dimensionality reduction technique in single-cell RNA-seq analysis. In each UMAP plot, every dot represents an individual cell, with colors indicating specific metadata attributes. For example, Figure 2 displays UMAP projections before and after batch effect correction using scVI. Cells are colored according to their respective batch. Notably, post-correction, cells from different batches appear more intermixed, suggesting effective removal of batch-specific technical variation while preserving meaningful biological structure in the data.

To evaluate the effectiveness of data integration, the Local Inverse Simpson's Index (LISI) was used, as adapted by [17]. The iLISI score quantifies batch mixing, ranging from 1 (no mixing) to B (complete mixing across B batches), and is normalized by scIB to a 0–1 scale, with higher values indicating better integration [17], [18]. After applying scVI, the LISI score increased from 0.057 to 0.38, reflecting a clear improvement in batch mixing. This quantitative result

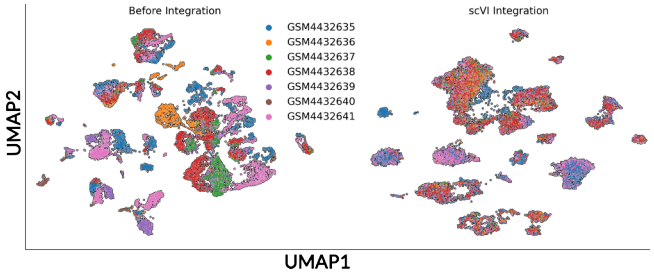

Fig. 2. UMAP projections of the dataset before and after batch effect correction using scVI. Each point represents a single cell, colored by its batch of origin. After correction, cells from different batches show increased mixing, indicating successful reduction of batch-specific technical variation while maintaining underlying biological structure.

supports the UMAP visualizations, confirming that scVI effectively minimized batch effects while preserving the biological structure of the data.

Leiden clustering was applied to the integrated dataset at a resolution of 0.25, resulting in 19 well-defined and, in some cases, distinct clusters. Cell-type annotation was performed using decoupleR alongside marker genes for human brain tissue from the CellRank 2.0 repository. Based on marker gene expression, seven cell types were identified, with a large proportion of cells classified as Excitatory Neurons. Figure 3 displays the clustering results (left) and corresponding cell-type annotations (right).

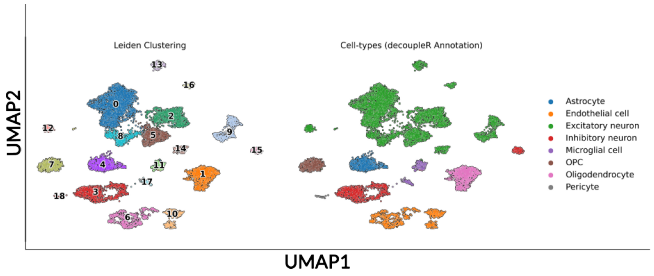

Fig. 3. UMAP visualization of cell clustering and annotation results. On the left, 19 cell clusters are shown following Leiden clustering at a resolution of 0.25. On the right, cell types were assigned using decoupleR with human brain marker genes from the CellRank 2.0 repository, revealing seven major cell populations. A large fraction of cells were identified as Excitatory Neurons, with additional populations including Astrocytes, Inhibitory Neurons, Microglial Cells, OPCs, Oligodendrocytes, Endothelial cells, and Pericytes.

Beyond the global analysis, focused investigations were performed on endothelial and pericyte cell populations to examine BBB-related molecular mechanisms with greater specificity. Following subsetting and reclustering, two transcriptionally distinct endothelial clusters and one pericyte cluster were identified. Differential expression and enrichment analyses within these populations revealed cell-type-specific molecular signatures potentially linked to BBB disruption in early Alzheimer's pathology. These results provide an additional layer of resolution, emphasizing the cellular heterogeneity underlying vascular dysfunction in the disease.

Differential expression analysis was performed using the Wilcoxon rank-sum test, applying a significance threshold of $p < 0.05$ and an absolute log fold change $|\log FC| \geq 1$ to identify statistically significant differentially expressed genes (DEGs). The results are visualized in a volcano plot (Figure 4), where each point represents an individual gene. Genes shown in light blue are significantly underexpressed in disease cells relative to controls, while those in red are significantly overexpressed. Genes in gray do not exhibit statistically significant expression differences between the two conditions.

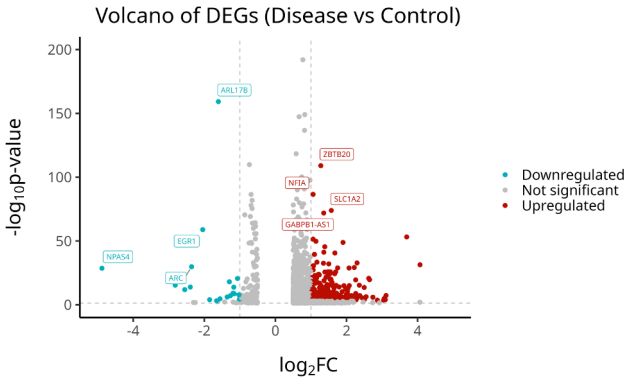

Fig. 4. Volcano plot illustrating the results of differential expression analysis using the Wilcoxon rank-sum test. Each point represents a gene, with light blue indicating significant underexpression in disease cells compared to controls, and red indicating significant overexpression. Gray points correspond to genes with no statistically significant expression differences between the two conditions. Thresholds were set at $p < 0.05$ and $|\log FC| \geq 1$.

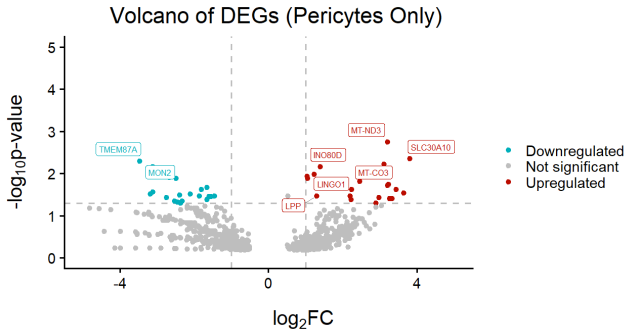

Fig. 5. Volcano plot illustrating the results of differential expression analysis using the Wilcoxon rank-sum test for pericyte cells only. Each point represents a gene, with light blue indicating significant underexpression in disease cells compared to controls, and red indicating significant overexpression. Gray points correspond to genes with no statistically significant expression differences between the two conditions. Thresholds were set at $p < 0.05$ and $|\log FC| \geq 1$.

Enrichment analysis of the top 100 differentially expressed genes was performed using the Enrichr platform, focusing on the BioPlanet 2019 pathway library. Among the most significant pathways, the BDNF signaling pathway was identified. Impaired BDNF (Brain-Derived Neurotrophic Factor) signaling via the TrkB receptor has been reported in the

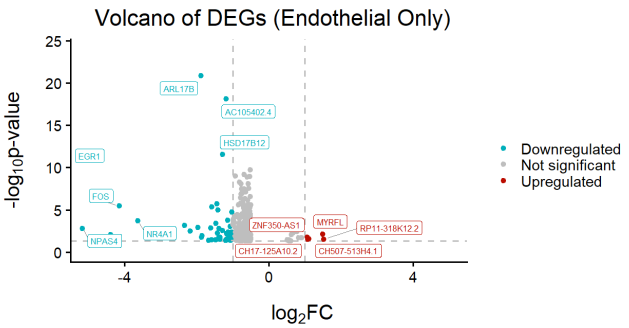

Fig. 6. Volcano plot illustrating the results of differential expression analysis using the Wilcoxon rank-sum test for endothelial cells only. Each point represents a gene, with light blue indicating significant underexpression in disease cells compared to controls, and red indicating significant overexpression. Gray points correspond to genes with no statistically significant expression differences between the two conditions. Thresholds were set at $p < 0.05$ and $|\log FC| \geq 1$.

early stages of Alzheimer's disease (AD), contributing to synaptic and neuronal loss as well as cognitive decline [19]. Although its direct involvement in amyloid or tau pathology remains unclear, reduced BDNF levels have consistently been associated with neurodegeneration in both human and animal studies.

Gene Ontology (GO) analysis of cellular components highlighted cell-cell junctions as the most significantly enriched category. These junctions are essential for maintaining structural integrity and signaling across the blood-brain barrier (BBB). Disruptions in tight, gap, and adherens junctions that are formed by proteins such as claudins, occludin, ZO-1, and VE-cadherin have been linked to increased BBB permeability and AD progression [20]. Additionally, the OMIM Disease library revealed age-related macular degeneration (AMD) as the most significantly associated condition. Recent studies report that individuals with AMD face a higher risk of developing AD, particularly at younger ages [21], supporting a possible shared pathological mechanism between retinal and neurodegenerative disorders.

In addition, GO analysis related to biological processes revealed that L-glutamate transmembrane transport was the most significantly enriched term. Dysregulation of glutamate transporters—key proteins responsible for maintaining glutamate homeostasis in the synaptic cleft—has been implicated in synaptic dysfunction and neurodegeneration in AD. Impaired clearance of excess glutamate may lead to excitotoxicity and contribute to progressive synaptic loss. Figure 7 illustrates the enrichment analysis results.

The top 42 DEGs of pericyte cells have been explored for enrichment, revealing significant alterations in pathways related to vascular function, DNA repair, and cellular stress responses. Enrichment in terms such as vasculature development and positive regulation of DNA repair suggests active vascular remodeling and genomic maintenance mechanisms in Alzheimer's pericytes. Processes involving p53-mediated

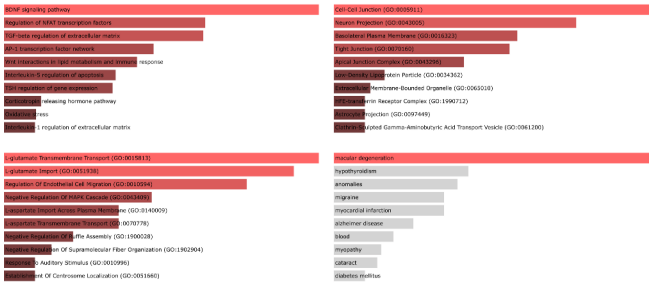

Fig. 7. Enrichment analysis of the top 100 differentially expressed genes using Enrichr highlighted key pathways and biological processes associated with Alzheimer's disease across all cell-types. Notable findings include the BDNF signaling pathway, cell-cell junction organization, and L-glutamate transmembrane transport. The OMIM Disease library further identified age-related macular degeneration as significantly associated with the gene set, suggesting potential links between retinal and neurodegenerative pathology.

signaling and miRNA regulation indicate stress-induced transcriptional control. The cellular component analysis showed strong associations with autolysosome, secondary lysosome, and ribosome, pointing to enhanced autophagic activity and protein synthesis. Overall, these results highlight a stressed yet adaptive pericyte phenotype, contributing to vascular dysfunction and impaired proteostasis in Alzheimer's disease (as shown in figure 8.

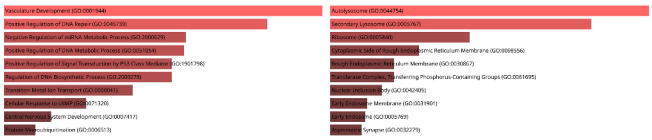

Fig. 8. GO enrichment analysis of the top 42 differentially expressed genes (DEGs) in pericyte cells from Alzheimer's patients compared to controls. The most enriched biological processes include vasculature development, DNA repair, and p53-mediated signaling, reflecting vascular remodeling and cellular stress responses. Enriched cellular components, such as lysosomal and ribosomal structures, indicate enhanced autophagic and protein synthesis activity, suggesting an adaptive but stressed pericyte state in Alzheimer's disease.

The top 26 DEGs of endothelial cells have been explored for enrichment, revealing key alterations in gene regulation and calcium-dependent signaling. Enrichment in positive regulation of gene expression via CpG island demethylation and regulation of calcium ion transmembrane transport suggests epigenetic modulation and disrupted calcium homeostasis in Alzheimer's disease. The cellular component analysis highlighted AMPA and ionotropic glutamate receptor complexes along with voltage-gated calcium channels, indicating endothelial involvement in neurovascular signaling. Together, these findings point to transcriptional reprogramming and altered calcium and glutamate signaling pathways that may contribute to endothelial dysfunction and impaired blood–brain barrier integrity in Alzheimer's disease (as shown in figure 9).

IV. Conclusion

AD is the primary cause of neurodegenerative dementia in older adults, characterized by progressive cognitive decline.

Fig. 9. GO enrichment analysis of the top 26 differentially expressed genes (DEGs) in endothelial cells from Alzheimer's patients compared to controls. Enriched biological processes involve gene expression regulation and calcium signaling, while cellular component terms highlight glutamate receptor and calcium channel complexes. These results suggest transcriptional and signaling alterations in endothelial cells that may underlie neurovascular dysfunction in Alzheimer's disease.

The complexity of the disease is amplified by its multifactorial nature, which includes genetic, environmental, and molecular factors. Investigating the pathogenesis of AD remains a challenge due to the brain's inherent diversity and the complex interactions among different cell types. In the present study, we analyzed snRNA-seq data derived from the entorhinal cortex of post-mortem samples, comparing individuals diagnosed with AD (Braak stage II) to healthy controls. Our findings revealed dysregulation of glutamate transporters and a significant enhancement of the BDNF signaling pathway, both strongly associated with synaptic dysfunction and neurodegeneration in AD.

Cell-type-specific analyses of endothelial and pericyte populations revealed key mechanisms of blood–brain barrier (BBB) dysfunction in AD. In pericytes, enrichment of genes linked to vascular development, DNA repair, and p53 signaling indicated an adaptive yet insufficient response to oxidative and genomic stress, contributing to vascular instability and neuroinflammation. Endothelial cells showed enrichment in calcium signaling and glutamate receptor complexes, suggesting disrupted calcium homeostasis and impaired neurovascular coupling. Together, these findings indicate that molecular alterations in both cell types converge toward BBB disruption and dysfunctional neurovascular signaling, reinforcing the link between vascular and neuronal pathways in AD and highlighting the value of cell-type-specific profiling for early detection and therapeutic targeting.

Acknowledgements

This work was carried out within the framework of the Action 'Flagship Research Projects in challenging interdisciplinary sectors with practical applications in Greek industry', implemented through the National Recovery and Resilience Plan Greece 2.0 and funded by the European Union – NextGenerationEU (project code: TAEDR-0535850).

References

[1] A. Association, "2019 alzheimer's disease facts and figures," *Alzheimer's & dementia*, vol. 15, no. 3, pp. 321–387, 2019.

[2] Y. L. Rao, B. Ganaraja, B. Murlimanju, T. Joy, A. Krishnamurthy, and A. Agrawal, "Hippocampus and its involvement in alzheimer's disease: a review," *3 Biotech*, vol. 12, no. 2, p. 55, 2022.

[3] K. M. Igarashi, "Entorhinal cortex dysfunction in alzheimer's disease," *Trends in neurosciences*, vol. 46, no. 2, pp. 124–136, 2023.

[4] W. Jin, J. Pei, J. R. Roy, S. Jayaraman, R. M. Ahalliya, G. V. Kanniappan, M. Mironescu, and C. P. Palanisamy, "Comprehensive review on single-cell rna sequencing: A new frontier in alzheimer's disease research," *Ageing Research Reviews*, vol. 100, p. 102454, 2024.

[5] L. Brase, S.-F. You, R. D. Albanus, J. L. Del-Aguila, Y. Dai, B. C. Novotny, C. Soriano-Tarraga, T. Dykstra, M. V. Fernandez, J. P. Budde *et al.*, "A landscape of the genetic and cellular heterogeneity in alzheimer disease," *MedRxiv*, pp. 2021–11, 2021.

[6] C. Zhang, G. Tan, Y. Zhang, X. Zhong, Z. Zhao, Y. Peng, Q. Cheng, K. Xue, Y. Xu, X. Li *et al.*, "Comprehensive analyses of brain cell communications based on multiple scrna-seq and snrna-seq datasets for revealing novel mechanism in neurodegenerative diseases," *CNS Neuroscience & Therapeutics*, vol. 29, no. 10, pp. 2775–2786, 2023.

[7] P. V. Kharchenko, "The triumphs and limitations of computational methods for scrna-seq," *Nature methods*, vol. 18, no. 7, pp. 723–732, 2021.

[8] K. Leng, E. Li, R. Eser, A. Piergies, R. Sit, M. Tan, N. Neff, S. H. Li, R. D. Rodriguez, C. K. Suemoto *et al.*, "Molecular characterization of selectively vulnerable neurons in alzheimer's disease," *Nature neuroscience*, vol. 24, no. 2, pp. 276–287, 2021.

[9] F. A. Wolf, P. Angerer, and F. J. Theis, "Scanpy: large-scale single-cell gene expression data analysis," *Genome biology*, vol. 19, no. 1, p. 15, 2018.

[10] G. X. Zheng, J. M. Terry, P. Belgrader, P. Ryvkin, Z. W. Bent, R. Wilson, S. B. Ziraldo, T. D. Wheeler, G. P. McDermott, J. Zhu *et al.*, "Massively parallel digital transcriptional profiling of single cells," *Nature communications*, vol. 8, no. 1, p. 14049, 2017.

[11] N. J. Bernstein, N. L. Fong, I. Lam, M. A. Roy, D. G. Hendrickson, and D. R. Kelley, "Solo: doublet identification in single-cell rna-seq via semi-supervised deep learning," *Cell systems*, vol. 11, no. 1, pp. 95–101, 2020.

[12] C. Xu, R. Lopez, E. Mehlman, J. Regier, M. I. Jordan, and N. Yosef, "Probabilistic harmonization and annotation of single-cell transcriptomics data with deep generative models," *Molecular systems biology*, vol. 17, no. 1, p. e9620, 2021.

[13] V. A. Traag, L. Waltman, and N. J. Van Eck, "From louvain to leiden: guaranteeing well-connected communities," *Scientific reports*, vol. 9, no. 1, pp. 1–12, 2019.

[14] P. Badia-i Mompel, J. Vélez Santiago, J. Braunger, C. Geiss, D. Dimitrov, S. Müller-Dott, P. Taus, A. Dugourd, C. H. Holland, R. O. Ramirez Flores *et al.*, "decoupler: ensemble of computational methods to infer biological activities from omics data," *Bioinformatics advances*, vol. 2, no. 1, p. vbac016, 2022.

[15] C. Hu, T. Li, Y. Xu, X. Zhang, F. Li, J. Bai, J. Chen, W. Jiang, K. Yang, Q. Ou *et al.*, "Cellmarker 2.0: an updated database of manually curated cell markers in human/mouse and web tools based on scrna-seq data," *Nucleic acids research*, vol. 51, no. D1, pp. D870–D876, 2023.

[16] Z. Xie, A. Bailey, M. V. Kuleshov, D. J. Clarke, J. E. Evangelista, S. L. Jenkins, A. Lachmann, M. L. Wojciechowicz, E. Kropiwnicki, K. M. Jagodnik *et al.*, "Gene set knowledge discovery with enrichr," *Current protocols*, vol. 1, no. 3, p. e90, 2021.

[17] I. Korsunsky, N. Millard, J. Fan, K. Slowikowski, F. Zhang, K. Wei, Y. Baglaenko, M. Brenner, P.-r. Loh, and S. Raychaudhuri, "Fast, sensitive and accurate integration of single-cell data with harmony," *Nature methods*, vol. 16, no. 12, pp. 1289–1296, 2019.

[18] M. D. Luecken, M. Büttner, K. Chaichoompu, A. Danese, M. Interlandi, M. F. Müller, D. C. Strobl, L. Zappia, M. Dugas, M. Colomé-Tatché *et al.*, "Benchmarking atlas-level data integration in single-cell genomics," *Nature methods*, vol. 19, no. 1, pp. 41–50, 2022.

[19] S. Kumari, R. Dhapola, and D. H. Reddy, "Apoptosis in alzheimer's disease: insight into the signaling pathways and therapeutic avenues," *Apoptosis*, vol. 28, no. 7, pp. 943–957, 2023.

[20] K. Asghari, Z. Niknam, S. Mohammadpour-Asl, and L. Chodari, "Cellular junction dynamics and alzheimer's disease: a comprehensive review," *Molecular Biology Reports*, vol. 51, no. 1, p. 273, 2024.

[21] L.-Y. Wen, L. Wan, J.-N. Lai, C. S. Chen, J. J.-Y. Chen, M.-Y. Wu, K.-C. Hu, L.-T. Chiu, P.-T. Tien, and H.-J. Lin, "Increased risk of alzheimer's disease among patients with age-related macular degeneration: A nationwide population-based study," *PLoS One*, vol. 16, no. 5, p. e0250440, 2021.